

2-18-2015

Ramsey method for Auger-electron interference induced by an attosecond twin pulse

Christian Buth
SLAC National Accelerator Laboratory

Kenneth J. Schafer
SLAC National Accelerator Laboratory

Follow this and additional works at: https://digitalcommons.lsu.edu/physics_astronomy_pubs

Recommended Citation

Buth, C., & Schafer, K. (2015). Ramsey method for Auger-electron interference induced by an attosecond twin pulse. *Physical Review A - Atomic, Molecular, and Optical Physics*, 91 (2) <https://doi.org/10.1103/PhysRevA.91.023419>

This Article is brought to you for free and open access by the Department of Physics & Astronomy at LSU Digital Commons. It has been accepted for inclusion in Faculty Publications by an authorized administrator of LSU Digital Commons. For more information, please contact ir@lsu.edu.



CHORUS

This is the accepted manuscript made available via CHORUS. The article has been published as:

Ramsey method for Auger-electron interference induced by an attosecond twin pulse

Christian Buth and Kenneth J. Schafer

Phys. Rev. A **91**, 023419 — Published 18 February 2015

DOI: [10.1103/PhysRevA.91.023419](https://doi.org/10.1103/PhysRevA.91.023419)

Ramsey’s method for Auger electron interference induced by an attosecond twin pulse

Christian Buth* and Kenneth J. Schafer

The PULSE Institute for Ultrafast Energy Science,

SLAC National Accelerator Laboratory, Menlo Park, California 94025, USA and

Department of Physics and Astronomy, Louisiana State University, Baton Rouge, Louisiana 70803, USA

We examine the archetype of an interference experiment for Auger electrons: two electron wave packets are launched by inner-shell ionizing a krypton atom using two attosecond light pulses with a variable time delay. This setting is an attosecond realization of Ramsey’s method of separated oscillatory fields. Interference of the two ejected Auger electron wavepackets is predicted indicating that the coherence between the two pulses is passed to the Auger electrons. For the detection of the interference pattern an accurate coincidence measurement of photo- and Auger electrons is necessary. The method allows one to control inner-shell electron dynamics on an attosecond time scale and represents a sensitive indicator for decoherence.

PACS numbers: 32.80.Hd, 32.80.Fb, 32.80.Aa, 32.70.Jz

Ramsey’s method of separated oscillatory fields [1, 2] represents a paradigm of precision measurement for various physical quantities. In its original conception for the measurement of nuclear magnetic moments, the scheme uses two coherent radiation fields, which are separated by a field-free propagation interval. The signature of the coherent interaction is the appearance of interference fringes when the physical quantity under consideration is measured at the exit of this experimental setup. Since Ramsey’s seminal studies, his method has been extended and modified extensively, e.g., by considering multiple fields with varying phase and amplitude and by applying it to masers and lasers [1]. The method of separated oscillatory fields is an interferometric approach which has the advantage over pump-probe schemes that it does not depend on an intense pump pulse [3].

In this paper, we propose a Ramsey scheme for attosecond science assuming two coherent pulses with a FWHM duration of $\tau_X = 500$ as each, which are separated by a variable delay of τ [Fig. 1] [4]. With an essential-states model [5, 6], we investigate the situation where a twin pulse ionizes the $3d$ shell of krypton atoms; the $3d$ holes subsequently decay in terms of an $M_{4,5}N_1N_{2,3}$ Auger process. In fact one of the first applications in attosecond science was the determination of the time constant of this Auger decay channel—a well-known datum from frequency-domain spectroscopy, $\tau_{3d} = 7.5$ fs—with a single attosecond pulse in the presence of an optical streaking laser [7]. Unlike this first investigation, our proposal of an attosecond Ramsey method [Fig. 1] represents a fundamental experiment which is only feasible with attosecond science and has no frequency domain equivalent in the sense that the attosecond twin pulse is crucial for its realization. Nonetheless, the spectra in this paper are shown in frequency domain. Furthermore, Auger de-

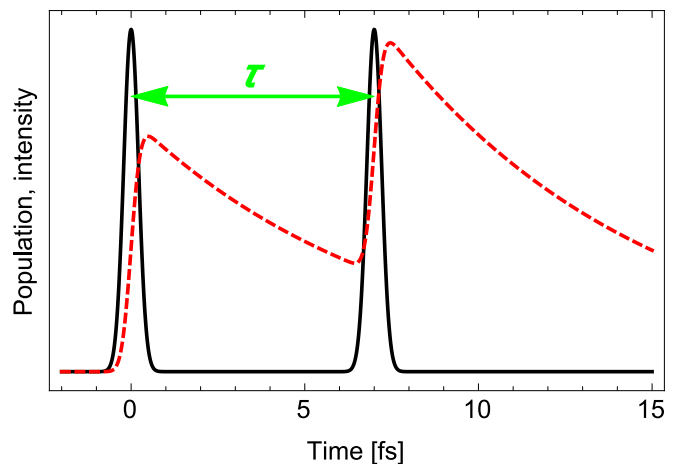


FIG. 1. (Color) The XUV intensity $I_X(t)$ (red) and krypton $3d$ hole population $\rho(t)$ (black) [Eq. (1)] for two attosecond pulses ($\tau_X = 500$ as) separated by a variable delay of τ .

cay [8] is a pure manifestation of electron correlations: it cannot be understood in terms of an effective one-electron model.

The twin pulse shown in Fig. 1 induces two outgoing photoelectron and Auger electron waves. Interference between two photoelectron wavepackets was examined in Ref. [9]. In that study, $5p$ Rydberg electrons of potassium atoms were subjected to two identical time-delayed laser pulses with a FWHM duration of 30 fs each at 790 nm wavelength and the resulting interference pattern in the photoelectron spectrum was analyzed. In contrast to the experiment in Ref. [9], we ask whether the coherence of the light is also transferred to the Auger electrons and what kind of Auger electron spectrum can we expect if it is? Clearly, for a time delay between the two pulses of $\tau = 0$ and of $\tau \rightarrow \infty$, we observe no interference fringes. What happens in between the two limiting cases? Clearly, our proposal of an attosecond Ramsey scheme represents an important experimental test of our

* Corresponding author. Present address: Theoretische Chemie, Physikalisch-Chemisches Institut, Ruprecht-Karls-Universität Heidelberg, Im Neuenheimer Feld 229, 69120 Heidelberg, Germany; christian.buth@web.de

understanding of Auger decay. Further, the scheme also represents a versatile tool for measurements. It enables one to precisely determine the position of Auger lines and it is a measure of coherence. Such an experiment would also address the following questions: how much decoherence is caused by the Auger process and what is the coherence time? Is our understanding of Auger decay complete?

The simplest way to describe Auger decay is shown in Fig. 1. Here, a rate-equation model which is used to determine the probability to find a $3d$ hole at time t in krypton $\varrho(t)$ [7]. It is given by the convolution of exponential Auger decay with a width of $\Gamma = 88$ meV [7, 10] with the XUV intensity

$$\varrho(t) = \frac{\sigma}{\omega_X} \int_{-\infty}^t I_X(t') e^{-\Gamma(t-t')} dt'. \quad (1)$$

The absorption cross section σ is taken to be constant over the bandwidth of the XUV pulse with a central angular frequency of ω_X and an intensity of $I_X(t')$ at time t' . The model does not honor the phase relationship between the two ejected Auger electron wave packets and thus does not describe interference effects [5].

To treat the quantum mechanical phases correctly, we use an *ab initio* formalism for the quantum dynamics of Auger decay of atoms which are inner-shell ionized by extreme ultraviolet (XUV) light [6]. The attosecond pulses of present-day light sources have a low peak intensity and its interaction may be described perturbatively as a one-photon process [3]. The quantum dynamics of the inner-shell hole creation with subsequent Auger decay is given by equations of motion which we simplify here in terms of an essential-states model [5, 6]. Our theory yields the probability density amplitude $\bar{c}_A^{\vec{k}_P \vec{k}_A}(\tau)$ to find a photoelectron with momentum \vec{k}_P in coincidence with an Auger electron with momentum \vec{k}_A for a delay of τ between the two pulses in Fig. 1. The probability density amplitude is adapted for no laser dressing from Eqs. (61) and (62) of Ref. [6]; it reads

$$\bar{c}_A^{\vec{k}_P \vec{k}_A}(\tau) = \frac{i}{2} \bar{d}(\vec{k}_P) \bar{v}(\vec{k}_A) S\left(\tau, \frac{\vec{k}_P^2}{2}, \frac{\vec{k}_A^2}{2}\right), \quad (2)$$

with the rms dipole and rms Auger decay matrix elements $\bar{d}(\vec{k}_P)$ and $\bar{v}(\vec{k}_A)$, respectively. The line shape function in Eq. (2) is

$$S(\tau, \omega_P, \omega_A) = \frac{\tilde{\varepsilon}_X(\tau, \omega_P + \omega_A - \Omega_P - \Omega_A)}{\omega_A - \Omega_A - \Delta_R + i\frac{\Gamma}{2}}; \quad (3)$$

it depends only on the absolute values of the momenta $k_P = |\vec{k}_P|$ and $k_A = |\vec{k}_A|$. Further, it contains the nominal photoelectron and Auger electron energies, which are in our case $\Omega_P = 20$ eV and $\Omega_A = 40$ eV, respectively [6]. In Eq. (3), Δ_R is the second-order energy shift and Γ is the Auger decay width [6]. The spectral

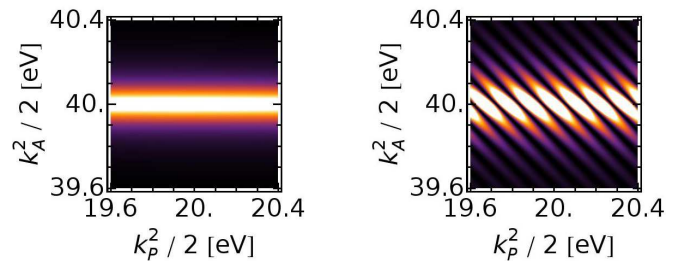


FIG. 2. (Color) Probability density $|\bar{c}_A^{\vec{k}_P \vec{k}_A}(\tau)|^2$ [Eq. (2)] to find a photoelectron with k_P and an Auger electron with k_A . We average the photoelectron over the full solid angle and view the Auger electrons along the z axis (linear XUV polarization axis). The left panel is for a delay of $\tau = 0$ and the right panel is for $\tau = 5 \tau_{3d}$. The color scale is linear.

envelope of the XUV light for a twin pulse is given by

$$\tilde{\varepsilon}_X(\tau, \omega) = \sqrt{\frac{\pi}{2 \log 2}} \varepsilon_{X0} \tau_X e^{-\frac{\omega^2 \tau_X^2}{8 \log 2}} (1 + e^{i\omega\tau}), \quad (4)$$

with the peak electric field strength ε_{X0} .

The main result of this study, the probability density $|\bar{c}_A^{\vec{k}_P \vec{k}_A}(\tau)|^2$ [Eq. (2)], is displayed in Fig. 2 for both no time delay between the two pulses of Fig. 1, i.e., a single pulse, and a time delay of $\tau = 5 \tau_{3d}$. The second choice for τ is somewhat arbitrary; the value of $5 \tau_{3d}$ is high enough to cause significant structure in the right panel of Fig. 2. This indicates interference effects that we would like to analyze in the following. The shape of the plots in Fig. 2 is determined by the absolute square of the line shape function (3) in a non-trivial way. Horizontally, along the $k_P^2/2$ coordinate, the width of the line profile is determined by the FWHM of $|\tilde{\varepsilon}_X(\tau, \omega)|^2$, which in our case is 3.7 eV. Vertically, along the $k_A^2/2$ coordinate, the extension is defined by the Auger decay width of 88 meV [7, 10]. In the case of $\tau = 5 \tau_{3d}$, we have a more involved dependence; overall, the contour has the shape of a skewed hyperbola with respect to k_A caused by the denominator squared in Eq. (3). For a deeper understanding of Fig. 2, we realize that the emission of an Auger electron is in fact a correlated two-electron process of photoionization and electronic decay. For such a process, we can exploit the energy balance [3, 11]:

$$\frac{\vec{k}_P^2}{2} + \frac{\vec{k}_A^2}{2} = \omega_X - I^{++}. \quad (5)$$

Here, I^{++} represents the double ionization potential of the dicationic final state of the atom. The balance (5) manifests in the argument of $\tilde{\varepsilon}_X$ in Eq. (3) and, consequently, it is reflected by the diagonal lines in the right panel of Fig. 2. Relation (5) is only exact for monochromatic XUV light with photon energy ω_X , i.e., a continuous wave source.

In a typical Auger electron spectroscopy experiment, the photoelectron is not observed. Hence we need to

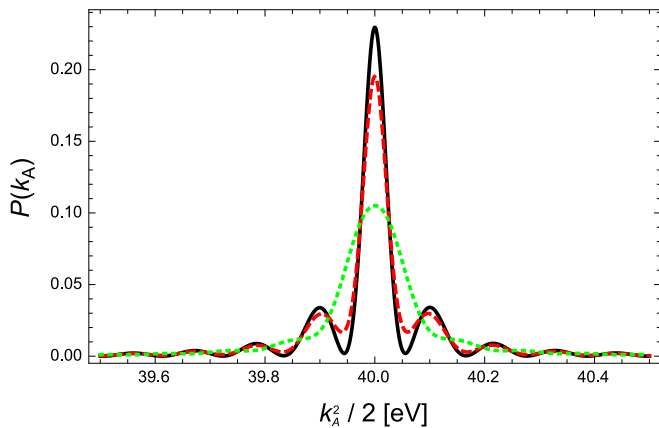


FIG. 3. (Color) Auger electron spectrum viewed along the z axis for an attosecond twin pulse with a separation of $\tau = 5\tau_{3d}$. The interference fringes are diminished for a decreasing accuracy of the photoelectron measurement; the energy uncertainties are: ± 0.04 eV (black), ± 0.1 eV (red), and ± 0.4 eV (green).

integrate the probability density (2) over the unobserved degrees of freedom, which is in this case the photoelectron momentum $\int |\tilde{c}_A^{\vec{k}_P, \vec{k}_A}(\tau)|^2 d^3k_P$. For each Auger electron momentum, this implies an integration along a horizontal line in Fig. 2. Following such a path in the right panel visually, we see that we average over many fringes with different energies which leads to a washing out of the interference pattern. Indeed, the resulting Auger electron spectrum exhibits no noticeable fringes for an unknown photoelectron momentum; it resembles closely the green curve in Fig. 3.

Inspecting the line shape function (3), we find that the XUV envelope is imprinted on the Auger electrons due to correlations between photoelectrons and Auger electrons. The finding that integrating over the photoelectron diminishes interference effects conforms to the general fact that summing over unobserved degrees of freedom generally comes with a loss of coherence. Consequently, to preserve the coherence of the Auger decay process, we need to take the photoelectron into account.

The other way round, however, does not hold true: it is *not* required to observe the Auger electron to see interference fringes in the photoelectron spectrum [9]. To see why this is so, we derive the probability density to observe a photoelectron. Within our formalism [6] it is given by

$$\tilde{P}_P(\vec{k}_P) = \frac{|\tilde{d}(\vec{k}_P)|^2}{2\pi} \int_{-\infty}^{\infty} \text{Im} \left[\frac{|\tilde{\varepsilon}_X(\tau, \omega)|^2}{\frac{\vec{k}_P^2}{2} - \Omega_P + \Delta_R - \omega - i\frac{\Gamma}{2}} \right] d\omega. \quad (6)$$

Our analysis has revealed the interconnection of the photoionization and the subsequent Auger decay; the dependence of Eq. (6) on the Auger decay width represents the reciprocal connection. This can be understood as

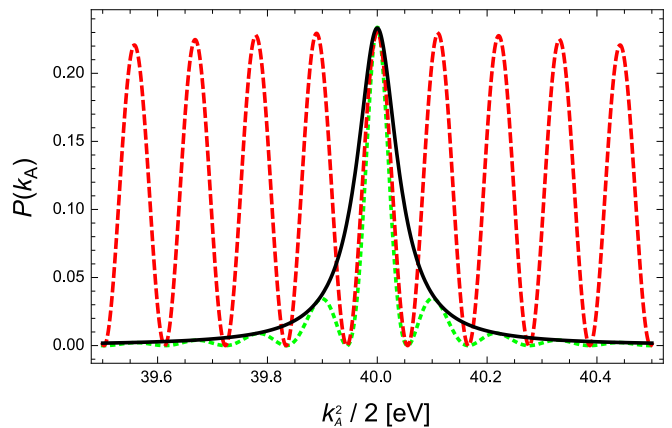


FIG. 4. (Color) Interference of the Auger electron waves (green) from an attosecond twin pulse for a precisely known photoelectron momentum $k_P^2/2 = \Omega_P$. The interference pattern is decomposed into the scaled line shape function (black) and the scaled XUV spectral envelope square (red, dashed).

follows: the interference of the photoelectrons is caused by the envelop $\tilde{\varepsilon}_X$ of the XUV light. The only impact of Auger decay on the photoelectron is due to the filling of the created hole which leads to a line broadening that leads for large Auger widths to a washing out of interference fringes.

To have a chance of observing interference between Auger electrons, we need to preserve the coherence of the Auger electron waves from the two XUV pulses. To accomplish this goal, we recall the energy balance in Eq. (5). It implies that if we measure the photoelectron momentum k_P with a certain precision, this defines the uncertainty in the Auger electron momentum k_A . In other words, if we restrict the allowed photoelectron momenta to a narrow range, the destructive interference of Auger waves should be reduced significantly. We integrate $|\tilde{c}_A^{\vec{k}_P, \vec{k}_A}(\tau)|^2$ over the full solid angle and a specified photoelectron momentum range Δk . This yields the probability $P_{PA, \Delta k}(\tau, k_P, k_A)$ to observe an Auger electron with k_A —we look along the z axis—for a photoelectron in the full solid angle with a momentum magnitude in the range of $[\max\{0, k_P - \Delta k\}; k_P + \Delta k]$. By integrating Eq. (6) over the same angular and momentum range, we find the normalized probability distribution of the photoelectrons $P_{P, \Delta k}(\tau, k_P)$ [6]; if we observe the photoelectron to lie in a chosen range, then the conditional probability to find an Auger electron with a specific momentum along the z axis $P_{A, k_P, \Delta k}(\tau, k_A)$ follows from Bayes law [12]:

$$P_{A, k_P, \Delta k}(\tau, k_A) = \frac{P_{PA, \Delta k}(\tau, k_P, k_A)}{P_{P, \Delta k}(\tau, k_P)}. \quad (7)$$

In Fig. 3, we investigate the Auger electron spectrum from Eq. (7). For a very accurate measurement of the photoelectron momentum (small uncertainty in Δk), we

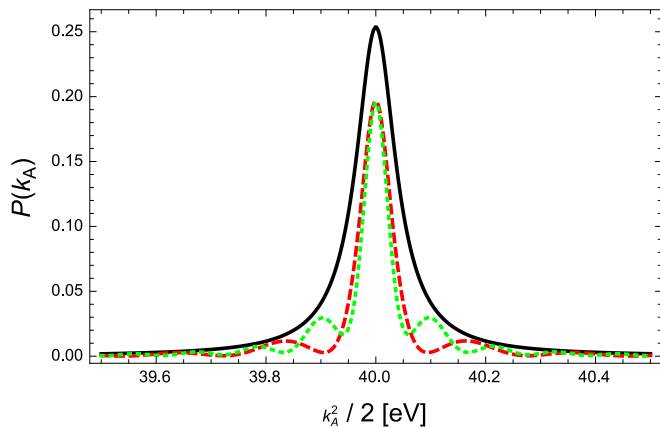


FIG. 5. (Color) Interference of the Auger electron wavelets for different time delays τ between the two attosecond pulses in Fig. 1: $\tau = 0$ (black), $\tau = 3\tau_{3d}$ (red), and $\tau = 5\tau_{3d}$ (green) for a photoelectron momentum which is known with an uncertainty of $(\Delta k)^2/2 = 10^{-5}$ eV.

find significant interference fringes. The interference effects are diminished with growing Δk , i.e., we average over Auger waves. The first maximum off the main peak in the curves of Fig. 3 moves to higher energies with increasing Δk .

In order to analyze the origin of the interference effects, we assume an exactly known photoelectron momentum magnitude and an exact detection of the Auger electrons along the z axis. In other words, we view the plots of Fig. 2 along a vertical line and normalize it to the peak of the photoelectron spectrum. In Fig. 4, we show a line-out of the right panel of Fig. 2 for $k_P^2/2 = \Omega_P$. The Auger electron spectrum is decomposed into a line-shape function and the spectral XUV pulse envelope (4) square. The line width only depends on the time delay τ as it should in Ramsey's method [1, 2] and the interference fringes in the XUV field envelope get thinner for increasing delay between the two pulses. The spectral width between the first minimum on the left and the first minimum on the right of the central peak of the fringes is $2\pi/\tau = 0.1$ eV

for $\tau = 5\tau_{3d}$.

For a system with decoherence, we assume that one will find a similar behavior of the interference pattern as for an inaccurately measured photoelectron momentum. In that case, in addition to averaging over wavelets with different wavelengths, also a jitter in the phase relation due to a coupling to other degrees of freedom in the system suppresses the interference fringes. Depending on the nature of the decoherence, a model of its impact on the signal can be made. Give a prediction of the signal the observed Auger electron interference pattern and its change, when the time delay τ in Fig. 1 is varied, can be used to identify and measure the amount of decoherence in a system. The impact of a variation of τ for our perfectly coherent case is revealed in Fig. 5. They resemble Fig. 3 in Ref. [9]. Thus an immediate application of the scheme discussed here is that it is a coherence meter.

The experimental investigation that we propose is challenging because a coincident detection of two electrons is necessary. In a recent experimental study [13], electrons from the KVV Auger decay of a $C1s$ vacancy in a CO molecule were measured in coincidence with the angular distribution of O^+ fragments. This technique can be used also in our case: the detection of the energy of the Auger electrons ejected along a specific direction in coincidence with the measurement of the momentum of the krypton ionic remnant offers an indirect pathway for a coincidence experiment for photo- and Auger electrons.

In this letter, we have proposed a fundamental experiment for studying the attosecond science equivalent of Ramsey's method of separated oscillatory fields: to what degree can we control an ultrafast electronic process in the time domain [3]? The setting can be used as a meter for decoherence in a system and offers interesting perspectives when used with intense XUV light tuned to an atomic resonance [14–16] where emission of a photoelectron can be avoided.

ACKNOWLEDGMENTS

This work was supported by the National Science Foundation grants No. PHY-0701372 and PHY-0449235.

[1] N. F. Ramsey, *Phys. Today* **33**, 25 (1980).
 [2] N. F. Ramsey, in *Nobel Lectures in Physics 1981–1990*, edited by G. Ekspong (World Scientific Publishing Company, Singapore, 1993) pp. 553–572.
 [3] F. Krausz and M. Ivanov, *Rev. Mod. Phys.* **81**, 163 (2009).
 [4] C. Buth and K. J. Schafer, *J. Phys.: Conf. Ser.* **194**, 022038 (2009), Proceedings for the XXVI International Conference on Photonic, Electronic, and Atomic Collisions (ICPEAC2009), July 22–28, 2009, Kalamazoo, Michigan, USA, arXiv:0905.2647.
 [5] O. Smirnova, V. S. Yakovlev, and A. Scrinzi, *Phys. Rev.*

Lett. **91**, 253001 (2003).
 [6] C. Buth and K. J. Schafer, *Phys. Rev. A* **80**, 033410 (2009), republished in *Virtual Journal of Ultrafast Science* **8**, issue 10 (2009), arXiv:0905.3756.
 [7] M. Drescher, M. Hentschel, R. Kienberger, M. Uiberacker, V. S. Yakovlev, A. Scrinzi, T. Westerwalbesloh, U. Kleineberg, U. Heinzmann, and F. Krausz, *Nature* **419**, 803 (2002).
 [8] P. Auger, *Compt. Rend. (Paris)* **177**, 169 (1923).
 [9] M. Wollenhaupt, A. Assion, D. Liese, C. Sarpe-Tudoran, T. Baumert, S. Zamith, M. A. Bouchene, B. Girard, A. Flettner, U. Weichmann, and G. Gerber, *Phys. Rev.*

- Lett. **89**, 173001 (2002).
- [10] M. Juvansuu, A. Kivimäki, and S. Aksela, Phys. Rev. A **64**, 012502 (2001).
- [11] O. Smirnova, V. S. Yakovlev, and M. Ivanov, Phys. Rev. Lett. **94**, 213001 (2005).
- [12] M. L. Boas, *Mathematical Methods in the Physical Sciences*, 2nd ed. (John Wiley & Sons, New York, 1983).
- [13] G. Prümper, H. Fukuzawa, D. Rolles, K. Sakai, K. C. Prince, J. R. Harries, Y. Tamenori, N. Berrah, and K. Ueda, Phys. Rev. Lett. **101**, 233202 (2008).
- [14] P. V. Demekhin and L. S. Cederbaum, Phys. Rev. A **86**, 063412 (2012).
- [15] B. W. Adams, C. Buth, S. M. Cavaletto, J. Evers, Z. Harman, C. H. Keitel, A. Pálffy, A. Picón, R. Röhlsberger, Y. Rostovtsev, and K. Tamasaku, J. Mod. Opt. **60**, 2 (2013), Special Issue: Physics in Quantum Electronics. Selected Papers from the 42nd Winter Colloquium on the Physics of Quantum Electronics, 2–6 January 2012.
- [16] A. Picón, C. Buth, G. Doumy, B. Krässig, L. Young, and S. H. Southworth, Phys. Rev. A **87**, 013432 (2013), arXiv:1302.0886.